

Thrust Bearing Load Observations in Deep Well Enclosed Lineshaft Pumps

Chris Reede¹, Dr. Haris Doumanidis², Dr. Matteo Aureli³, and Marie Curie²

¹Ormat Technologies

²Mechanical Engineering, Khalifa University, Abu Dhabi, UAE

³University of Nevada, Reno

Keywords

Well pumps, lineshaft pumps, axial thrust, geothermal production pumps, relative stretch

ABSTRACT

This paper reports the experimental observations of thrust bearing load on deeply set enclosed lineshaft pumps operating at various shaft speeds. In an effort to validate the accuracy of techniques commonly used to estimate such loads, a load cell was installed between the lineshaft connection and the motor thrust bearing of two identical make and model pumps. The first pump operated with an open lineshaft in the manufacturer's test lab and the second pump operated in the field with an enclosed lineshaft. The load cell allowed for real-time online measurement of impeller down-thrust encountered on the surface. The thrust measurements were normalized into thrust coefficients and plotted on curves, also known as K_t curves, for various shaft speeds. At lower speeds, it is observed that both the lab pump and field pump K_t curves are in agreement. However, the curves begin to diverge as shaft speed is increased above 1,600 RPM. More specifically, K_t curves measured in the field at 1,320 RPM closely followed those measured in the lab, while K_t curves taken in the field at 2,200 RPM were up to 58% lower than the lab measured curves. The experimental data indicate that motor thrust bearings on pumps operating at the usual speed of 1,800 RPM may be loaded significantly less than expected. As a consequence, the impeller relative movement, with respect to pump bowls, may be significantly less than expected. Overall, the data represent a comparison between a well-established lab-tested K_t curve and the K_t curve of a single pump running in the field. Repeatability of the findings needs to be further validated through testing of additional field pumps. Further modeling is also necessary to understand and model the up-thrust mechanisms present in the enclosing tube. Such further validation is expected to highlight general conclusions, allowing for the formulation of useful correlations which account for thrust error. Such correlations will allow operators of similar pumps to better determine motor thrust bearing loads and impeller movement to ultimately increase the production of fluid on the surface.

1. Introduction

Deeply set enclosed lineshaft driven vertical centrifugal pumps are utilized in the production wells at many geothermal power plants and direct use facilities. These pumps serve to increase the pressure and flow rate of brine produced to the surface. Often times, pumping of every production well in a field is necessary to make operation of a facility commercially viable. This is especially true if a facility is designed to handle the geothermal fluid exclusively in the liquid phase.

The usefulness of an installed production pump is directly proportional to the additional amount of fluid it can bring to the surface when compared to artesian flow of the well in question. The dependence of commercial viability on pump capacity often leads plant operators to place pumps in service on the far edges of their specified design limits. This emphasis on pump capacity also offers an incentive for manufacturers to make technological advances which lead to increased production.

In some cases, the amount of estimated impeller thrust may increase the estimated impeller movement relative to the pump bowls beyond values which the pump operator is comfortable using. In an effort to increase the operating clearance between the pump impellers and bowls, an operator may decide to reduce the expected relative impeller movement by installing a pump with less stages or run the same pump at a slower shaft speed. The actions taken to reduce relative stretch also result in diminished production capacity, making operation of the pump less profitable.

It is the purpose of this research to examine a commonly practiced method for determining impeller movement which uses the pit tested thrust coefficient to estimate both motor thrust bearing load and line shaft tension. To this aim, a non-contact load cell was used to measure the lineshaft tension at the motor thrust bearing of two pumps, both the same make and model (“subject pump”). The first pump was operated in the manufacturer’s test lab and driven by an open lineshaft. The second pump was operated in a well and driven by an enclosed lineshaft. Thrust measurements were taken over a range of flows at three shaft speeds in the lab and 10 shaft speeds in the field. The resulting measurements were normalized into easily comparable thrust coefficient curves.

It was observed that the field thrust coefficient curves began to significantly diverge from the test pit curves above a shaft speed of approximately 1,600 RPM with error between the lab and field tests increasing dramatically as shaft speed increased. The experimental data indicate that motor thrust bearings on pumps operating at the usual speed of 1,800 RPM may be loaded significantly less than expected. As a consequence, the impeller relative movement, with respect to pump bowls, may be significantly less than expected. The most likely cause for the very significant reduction in surface lineshaft tension is an upward force placed on the lineshaft inside the enclosing tube, possibly due to the viscous interaction between the lineshaft and lubricant at each bearing in the enclosing tube.

2. Field Experimentation

The following section outlines the equipment and procedure used to take thrust measurements on an enclosed lineshaft pump in service delivering geothermal fluid to an operating geothermal power plant.

2.1. Field K_t Measurement

The field test was conducted on a pump set 705 feet deep producing fluid to the Don A. Campbell geothermal power plant in Mineral County, Nevada. For the field experiment, shaft rotation was first fixed at a given speed. Then, the discharge valve was incrementally closed in order to increase discharge pressure, thus demanding higher head on the down-hole pump. The minimum pump outlet pressure was governed by the plant production header pressure. Efforts were made to lower the plant inlet pressure as close to the brine flash pressure as possible. A pressure margin was kept in place to prevent localized flashing across the throttling valve and downstream obstructions.

For each speed, a sufficient number of points were taken to infer the behavior of the K_t vs. flow curve (an average of 6 data points for each of the 11 curves taken). After a curve was taken for an individual shaft speed, the shaft speed setting was changed and a new curve was created by incrementally opening or closing the pump discharge valve.

Figure 1 displays a schematic of the test setup utilized for taking thrust measurements on a lineshaft pump operating in the field.

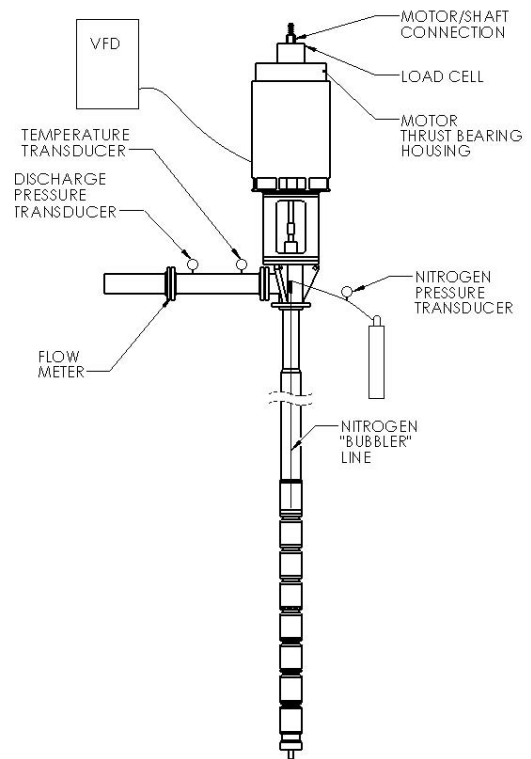


Figure 1. Field experiment test setup.

2.2. Field Experimental Instrumentation

Pump Shaft Speed Measurement

Pump shaft speed was measured through the use of a Nova-Strobe bbx Monarch hand-held calibrated photo tachometer shown on the exposed section of shaft between the motor and the mechanical seal.

Pump Suction Pressure Determination

The pump suction pressure P_s , measured in PSI, was determined using a 0.250 inch outer diameter, 0.049 inch wall thickness tube run from the suction of the pump to the surface. The tube, commonly referred to as a “bubbler” was filled with nitrogen. The bubbler tube pressure read on the surface P_b , also measured in PSI, is equal to the suction pressure minus the weight of nitrogen from the gauge to the bubbler tube depth D_b , measured in feet, per unit cross sectional area of the

tube inner diameter. Equation (1) can be used to find suction pressure given the bubbler pressure P_b and the temperature T , measured in degrees Fahrenheit of the produced fluid. Nitrogen was assumed to be an ideal gas with a compressibility factor of 1, see references [1, 4].

$$P_s = P_b + D_b \left(\frac{0.0727}{144} \right) \left(\frac{P_b + P_{atm}}{14.70} \right) \left(\frac{528}{T + 460} \right) \quad (1)$$

Here, the coefficient 0.0727 represents the density of nitrogen measured in lb/ft³ at 528°R and 14.7 PSI, 144 is a conversion factor from lb/ft³ to PSI/ft. The 14.7 and 528 constants represent the standard pressure and temperature in PSI and °R respectively. The addition of the constant 460 converts temperature measured in °F to °R. Pump bubbler pressure was measured in PSI using a Yokogawa model number EJA530E-JCS4N-017EL/FU1 calibrated pressure transducer tied to the bubbler at the surface.

Pump Flow Measurement

Flow was measured using a calibrated General Electric model number XMT8681-21-00-0011-0 ultra-sonic flow meter placed in the straight section of pipe several feet from the pump discharge.

Fluid Temperature Measurement

Brine temperature was measured using a calibrated PR Electronics model number 5333-B temperature transducer placed in a thermowell mounted on the discharge pipeline a few feet from the pump discharge head.

Pump Discharge Pressure Measurement

Pump discharge pressure P_d was measured through the use of a calibrated Yokogawa model number EJA530E-JCS4N-017EL/FU1 pressure transducer tied into the surface discharge pipeline a few feet from the pump discharge.

Column Head Loss Determination

Column head loss was determined using the Darcy-Weisbach friction factor which can be found in reference [2], among many other sources.

Specific Gravity Correlation

Specific gravity was corrected for temperature using a 4th order polynomial regression of water density vs. temperature values from reference [1].

Total System Head Determination

The total system head H was determined using equation (2) below, based on the volumetric flow reading measurement, wetted cross-sectional areas of the wellbore at the suction A_s and discharge A_d , measured in feet squared, suction pressure P_s , discharge pressure P_d , measured in PSIG, as well as column depth measured in feet D_c [3].

$$H = \frac{P_d - P_s}{0.4332 \cdot SG} + h_f + \frac{Q}{1.2963 \times 10^7 (A_d^2 - A_s^2)} + D_c \quad (2)$$

Here, h_f and SG are friction head measured in feet and specific gravity measured against water at standard imperial conditions.

3. Laboratory Experiment

The following section outlines the equipment and procedure used to take thrust measurements on an open lineshaft pump operating in the manufacturer's test pit pumping ambient temperature water.

3.1. Laboratory K_t Measurement

For each pump, pump head demand was varied through use of a remotely operated throttling valve, ultimately producing flows from shutoff to cavitation. Data were gathered through the use of a central data acquisition system, save for the load cell output, which was read through the digital display and recorded manually.

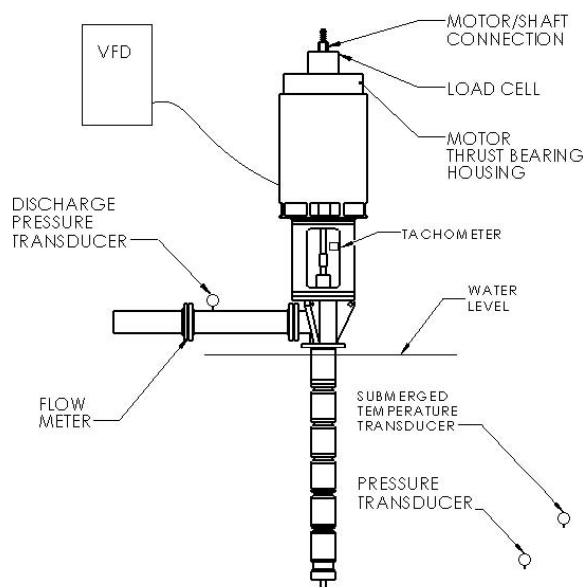


Figure 2. Lab experiment test setup.

3.2. Laboratory Experimental Instrumentation

Pump Suction Pressure Determination

Total system head was determined based on the static water level of the pit, eliminating the need to measure pressure at the pump suction. The pit level was measured using a Flowline® EchoSpan Model LU81/83/84 ultrasonic level transmitter.

Pump Flow Measurement

Flow was measured using the differential pressure across a B.I.F. Industries 8 inch universal Venturi tube mounted on the discharge pipe flow. The differential pressure was measured with a calibrated Rosemount 3051S1CD4A2E12A1AD1 model pressure transducer.

Pump Discharge Pressure Measurement

The lab pump discharge pressure was measured using a calibrated Omega PX-309 pressure transducer mounted on the outlet pipeline.

Pump Shaft Speed Measurement

The lab pump shaft speed was measured using a calibrated Monarch Instrument remote optical sensor (ROS) coupled to an adjustable magnetic base.

Column Head Loss Determination

The lab pump had no column; it was mounted directly to the discharge head.

Pit Water Temperature Measurement

The pit water temperature was determined using an Omega model HSTC-TT-J-20S0120 hermetically sealed and calibrated temperature transducer.

Specific Gravity Correlation

Specific gravity was corrected for temperature using a 4th order polynomial regression of water density vs. temperature values from reference [1].

Total System Head Measurement

Total system head H was determined using equation (3) below, where Q is the volumetric flow measured in GPM, L_w is the vertical distance from the water level to the pump discharge pipe centerline, measured in feet, and P_d is the discharge pressure measured in PSI. Both column and discharge head losses were neglected.

$$H = L_w + \frac{P_d}{0.4332 \cdot SG} + \frac{Q}{1.2963 \times 10^7 A^2} \quad (3)$$

where the coefficient 0.4332 is the pressure gradient of fluid at a specific gravity of 1.

4. Test Data

Data taken during the field and pit tests are reported in figures 3, 4, and 5. In these figures, marker color begins with dark blue for the lowest plotted shaft speed (1,320 RPM) and turns warmer as speed increases, ultimately becoming bright red for the highest speed plotted (2,200 RPM). Marker color is kept identical for speeds varying less than 10 RPM throughout the plots in this section. Round markers are used for the lab test data and diamond markers are used for field test data.

5. Discussion

5.1. Lab Experiment Discussion

Thrust coefficient curves were compiled from lab tests at three shaft speeds, shown in figure 3. The lab curves suggest that changes in pump shaft speed in the range of 1,320 to 1,785 RPM have little effect on the overall thrust coefficient value. All three curves approximately follow a similar upward-sloping parabolic curve with slight variation. The values taken at the highest speed of 1,790 RPM are not significantly larger than those taken at the lowest speed of 1,320 RPM.

Equation (4) below was determined using a second order polynomial regression of the lab-tested K_t values from 0 to 2,500 GPM. The resulting model is superimposed on the lab test readings in figure 3 (red curve). For typical downhole pump installations, equation (4) would be used to approximate impeller down force, motor thrust bearing load and the resulting impeller movement.

$$LabK_t = 3.714 \times 10^{-7} Q^2 + 2.068 \times 10^{-4} Q + 13.19 \tag{4}$$

5.2. Field Experiment Discussion

Figure 4 above displays the thrust coefficient curves from data obtained at 10 separate speeds on the same pump in three sessions. Data were taken twice at 1,782 RPM on separate dates. The plotted curves suggest that the thrust coefficient value decreases significantly as speed increases.

For a constant flow of 2,230 GPM, the data indicated a thrust coefficient decrease of more than 50% between the speeds of 1,289 RPM and 2,046 RPM. The significant decrease in shaft thrust at the surface for the same flow at higher speed suggests the presence of a significant error if the 1,785 RPM lab tested curve is used to directly approximate motor thrust bearing load and line shaft tension for a pump operating at a higher speed such as 2,200 RPM.

5.3. Comparison Between Lab and Field Tests

Figure 5 plots both the field and lab data on the same chart. While both the lab and field thrust coefficient curves taken at 1,320 RPM tend to agree with one another, the pairs of 1,630 RPM and 1,785 RPM curves are significantly far apart from each other. Comparison suggests the presence of large error between impeller down force on the motor thrust bearing in the lab versus field measurements at standard operating speeds, which are usually at or above 1,790 RPM.

6. Analysis of the Error

6.1. Error Determination

In order to quantify the error caused by approximating motor thrust bearing load with the lab tested curve given in equation (4), a percent error between the lab and field-measured values was calculated using equation (5) below. This percent error was calculated using the regression curve in equation (4) for every field measured thrust coefficient value and plotted in figure 6.

$$\%error = \frac{LabK_t - Field\ Read\ K_t}{Field\ Read\ K_t} \tag{5}$$

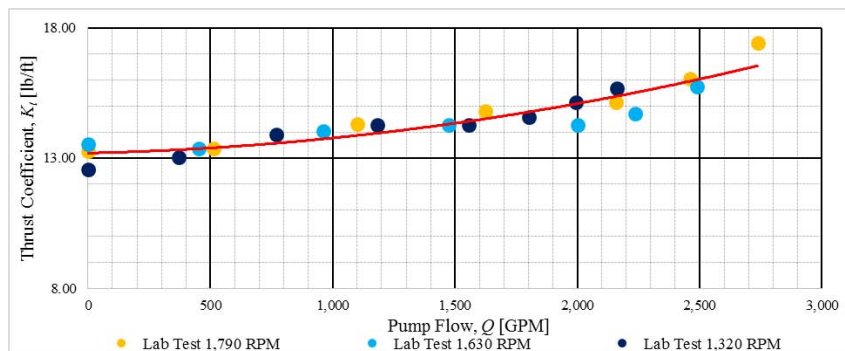


Figure 3. Lab measured K_t curves with second-order polynomial regression. Data refer to the 5 stage subject pump, operating in a test pit, directly coupled to discharge head with open lineshaft

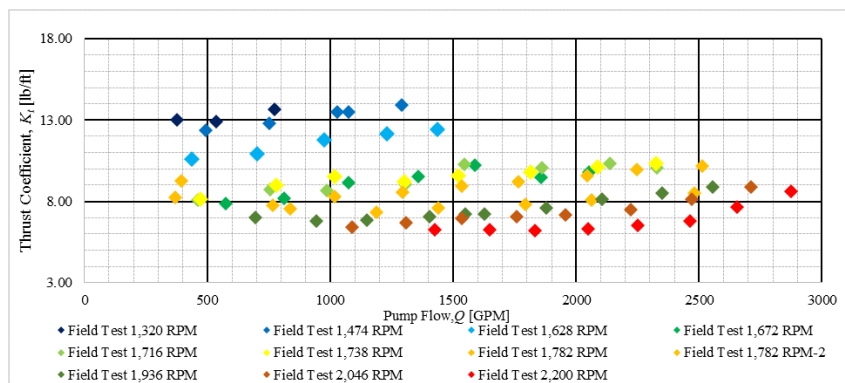


Figure 4. Field measured K_t vs. flow curves. Data refer to the 7 stage subject pump, 705' column depth, 10-3/4"-40.5lb/ft column pipe, 4" enclosing tube OD.

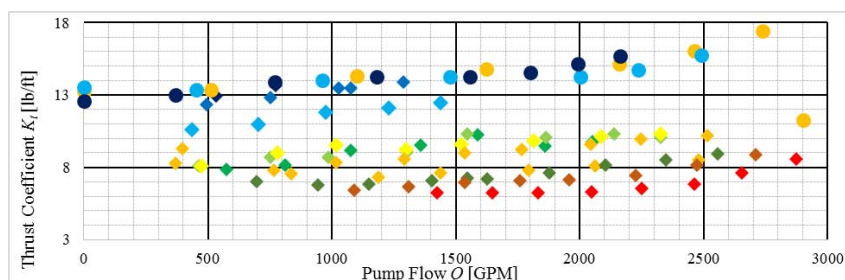


Figure 5. Lab and field tested K_t vs flow curves.

The percent error is displayed in figure 6 with red markers. Note that maximum discrepancies are up to the order of 150% for the largest shaft speeds tested.

6.2. Error Correction

In an effort to correct the lab test data, the correction factor outlined in equation (6) was used on thrust coefficient readings taken above 1,600 RPM.

$$Corrected K_t = Lab K_t \times \left(\frac{N}{1,300} \right)^{1.6} \tag{6}$$

Utilizing this correction reduced the error to a more manageable level, generally well below 20% throughout the entire range of shaft speeds. Results of this procedure are displayed in figure 6 with green markers. The 1,300 and 1.6 values in equation (6) were chosen through a “guess and check” iteration to minimize total error of the corrected values. Corrected error increases with pump flow, suggesting a second correction factor dependent upon the flow may be successful in further reducing error.

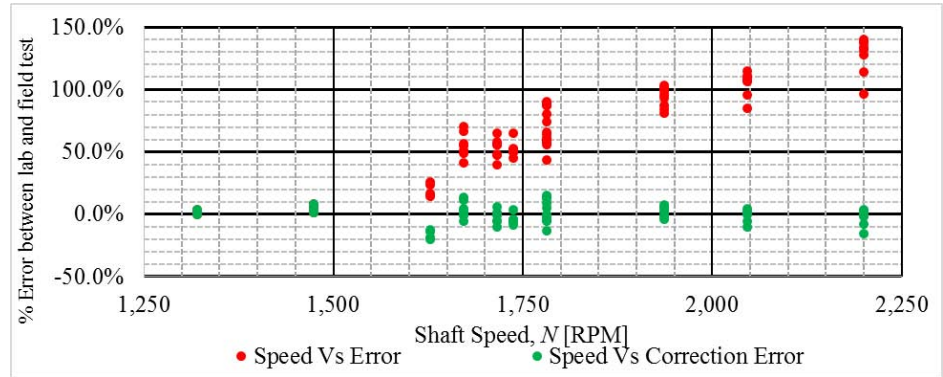


Figure 6. Direct and corrected percent error.

6.3. Repeatability

Two thrust coefficient vs. flow curves were collected at 1,782 RPM on separate days. The resulting curves are plotted below in figure 7. These two curves suggest that thrust may fluctuate over time, as there is definite scatter between them. The overall shape of both curves is similar. At the far right of the first test, the K_t value was 8.5lb/ft at 2,480 GPM while second test had a K_t value of 10.2lb/ft at 2,513 GPM for the second test. The difference between these two points represents an approximate change of 20% in the thrust value at similar duty points.

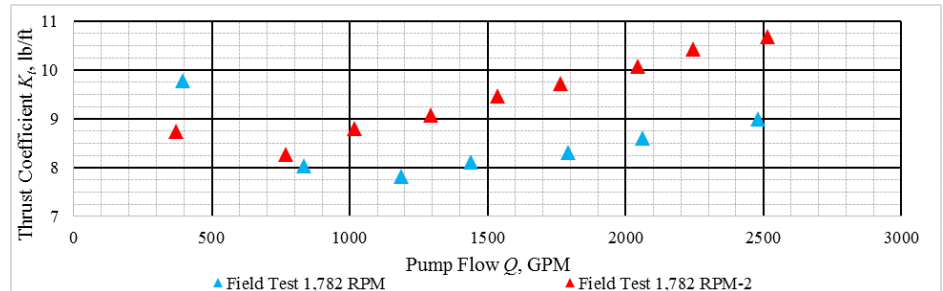


Figure 7. Field measured K_t curves taken at the same speed on separate days.

7. Possible Causes of Discrepancy

There is no reason to suspect any difference in impeller thrust actually developed by the down-hole pump assembly. This means that any discrepancy between the lab-tested K_t curve and the field measured K_t curve is most likely caused by up-thrust generated in the lineshaft and enclosing tube, as this is the only major difference between the two pump configurations. Below are the two most likely mechanisms for up-thrust generated in the pump lineshaft.



Figure 8. Signs of column contact on lineshaft enclosing tube.

7.1. Lineshaft Binding

Because most wellbores are not perfectly straight, it is reasonable to assume that the lineshaft will encounter slight to moderate bending along its path from the surface to the pump. The presence of bending has been confirmed multiple times through the presence of flat spots on the lineshaft enclosing tube. These flat spots have relieved sections corresponding to the column pipe coupling gaps. Figure 8 shows marks found on actual lineshaft enclosing tubes used in the field.

The effect of lineshaft binding is often neglected in the relative stretch calculations as the exact wellbore geometry may be unknown and modeling requires complex analysis. It is reasonable to expect the effect of binding to act as a constant friction-related up-thrust value, lowering the impeller down-thrust evenly across all flows.

7.2. Pumping Effect of Helical Grooves

The thrust coefficient correction factor used in equation (6) shows a strong dependence of measured down-thrust on shaft speed. Reference [5] suggests the presence of a pressure increase across helically-grooved bearings due to viscous friction. Each lineshaft bearing has two $\frac{3}{16}$ inch radius, 540° semi-circular spiral grooves running along the internal diameter, making them similar in geometry to the pumps studied in reference [5].

In the last few years, many deep well pumps have been put into service with welded discharge case bypass ports. A pump operating with welded bypass ports will have identical pressure at the discharge case on both the inner column wetted diameter and the inner enclosing tube wetted diameter. The pumps with welded bypass ports were originally expected to have more surface pressure in the enclosing tube than the discharge pipeline. The increased pressure was expected because the lineshaft lubricant has a lower density than the pumped fluid, making the hydraulic weight of oil lighter than the hydraulic weight of brine in the column pipe. In reality, when the pumps with welded bypass ports are started, the enclosing tube pressure at the surface is often less than atmospheric, indicating a strong pumping effect inside the enclosing tube.

Reference [5] states that the magnitude of any pressure added to the fluid flowing across the bearings increases exponentially with an increase in the peripheral speed of the shaft face. The low efficiency of such a pump geometry (less than 3%) suggests significant energy losses to the surroundings. It may be possible that a portion of the viscous force imparted on the lubrication fluid from the shaft reacts in the axial direction, placing an upward force on the lineshaft.

If the total discrepancy between the thrust measured in the test pit and the thrust measured on the field pump were to be attributed entirely to the pumping effect of bearings, as a first approximation, it is possible to hypothesize a uniform distribution of these forces across each bearing. It is assumed therefore, that the thrust discrepancy is given by the sum of equal upward forces applied to the shaft at the center of each of the enclosing tube screw bearings. In this simplified scenario, each of the 144 bearings from the surface to the pump discharge would need to apply 35 pounds of force to the shaft to account for the error seen between the 1,785 RPM lab tested thrust curve and the 2,200 RPM field tested thrust curve. However, the test method used in this paper cannot determine how the up-thrust is distributed across the lineshaft. Therefore, it is important that the up-thrust mechanism be further investigated.

8. Conclusions

The work described in this paper served to test the accuracy of an industry accepted method for determining surface lineshaft tension on enclosed lineshaft vertical deep well pumps. A non-contact load cell was used to measure the lineshaft tension at the motor thrust bearing of two pumps, both the same make and model. The first pump was operated in the manufacturer's test lab and driven by an open lineshaft. The second pump was operated in a well and driven by an enclosed lineshaft. Thrust measurements were taken over a range of flows at three shaft speeds in the lab and 10 shaft speeds in the field. The resulting measurements were normalized into easily comparable thrust coefficient curves and plotted in figure 5.

It was observed that the field thrust coefficient curves began to significantly diverge from the test pit curves above a shaft speed of approximately 1,600 RPM with error between the lab and field tests increasing dramatically as shaft speed increased. The most likely cause for the very significant reduction in surface lineshaft tension is an upward force placed on the lineshaft inside the enclosing tube. It is possible that the viscous interaction between the lineshaft and lubricant may be placing an upward force at each bearing in the enclosing tube. The presence of viscous upward force needs to be independently verified through additional empirical testing on the surface or numerical analysis.

This research identified an unexpected force which is not typically accounted for when determining lineshaft tension of an enclosed lineshaft pump. If the physical mechanism driving the identified upward force can be explained and accurately modelled, it would allow operators of this type of pump to set their pump impellers lower relative to the pump bowls. The lower impeller settings will allow operators to set pumps deeper than previously thought possible with existing equipment. Deeper pump settings will result in higher amounts of available well drawdown which, in some cases, can immediately be used to produce more fluid to the surface, allowing the pumps to generate more revenue.

In order to determine the thrust behavior of the enclosed lineshaft, it is necessary to model the viscous interaction between the shaft and helical bearing grooves, as for example indicated in [5]. This can be done both empirically through

the use of a scale model operated in a test lab, and analytically through the use of finite element modeling and computational fluid dynamic analysis. Once a reasonably accurate correlation enclosing tube up-thrust can be quantified, it can be compared to the field measurements reported in this paper.

Axial thrust measurements can also be taken on pumps of varying setting depth in an effort to quantify the effect of lineshaft length or number of bearings on the difference between expected and actual thrust. The net amount of up-thrust per bearing can also be identified and compared to the values found in this paper. As more and more empirical, experimental, and computational evidence is gathered, it is expected that these correlations may find extensive use in the design of geothermal deep well enclosed lineshaft pumps.

References

- [1] Çengel Y.A. and M.A. Boles, 2008. "Thermodynamics: an engineering approach." McGraw-Hill, Boston, MA. p. 134-139, 972.
- [2] Fox R.W., P.J. Pritchard, and A.T. McDonald, 2009. "Introduction to fluid mechanics" J. Wiley, p. 280, 330-332.
- [3] Heald C.C., 2002. "Cameron Hydraulic Data" Flowserve p. 1-7 – 1-12.
- [4] Jensen J.E., W.A. Tuttle, R.B. Stewart, H. Brechna, and A.G. Prodell, 1980. "Brookhaven National Laboratory selected cryogenic data notebook." BNL 10200-R, Vol. I. Chapter VI, Properties of Nitrogen, Table P V1-C-1.
- [5] Ludwig L.P, T.N. Strom, R.L. Johnson, 1969. "Experimental study of pump and seal characteristics of helical groove geometry incorporated in a combined bearing and pump" NASA Technical Note, p. 12.